

창립
40주년 학술대회
논문 87-K-20-3

NOA81 Optical Adhesive 를 중간층으로 하는 비선형 Etalon 에서 나타나는
광상안정현상에 대한 연구

공홍진, °황월연, 이상수
한국과학기술원 물리학과

Optical Bistability in Nonlinear Etalons Filled
with NOA81 Optical Adhesive

Hong Jin Kong, Wol Yon Hwang, and Sang Soo Lee
Dept. of Physics, Korea Advanced Institute of Science Technology

ABSTRACT

We have observed the optical bistabilities at 5145\AA in nonlinear etalons filled with NOA81 optical adhesive which is cured with UV light under the temperature gradient of $7^\circ\text{C}/\text{mm}$ on the NOA81 layer surface. The critical switch-on irradiance and switch-on time are $17\text{ KW}/\text{cm}^2$ and $350\mu\text{sec}$, respectively.

The switching contrast of up to 8 observed in NOA81 etalons is higher than that of ZnS or ZnSe interference filter, and the thermo-optic coefficient (dn/ndT) of NOA81 is measured to be at least $-3.8 \times 10^{-4}/^\circ\text{C}$ which is larger in magnitude than that of ZnS or ZnSe.

I. Introduction

Optical bistability has been investigated in a number of materials because of its potential application to optical logic gates. Thermally induced optical bistabilities have been mainly studied in the narrow-band pass filters containing ZnS or ZnSe active spacer¹. Because of their room temperature, visible wavelength, and low power operation characteristics, and the availability of large area for two dimensional parallel processing, they have attracted much attentions, and indeed many previous works have verified that the devices could be used in optical logic operation^{1,2,3}. In our experiment, we

have observed the optical bistabilities in nonlinear etalons filled with NOA81 optical adhesive (Norland Products Inc.).

It is UV-cured under specific temperature gradient. The device properties of NOA81 etalons are comparable to ZnS and ZnSe interference filters in many aspects, i.e. it operates at room temperature under visible wavelength cw laser beam illumination, at low switch-on power level, and has high switching contrast.

II. Devices description

While NOA81 filled in between two dielectric mirrors is being UV-cured, the temperature gradient of $7^\circ\text{C}/\text{mm}$ is maintained on the NOA81 layer surface as shown in Fig.1. NOA81 etalons prepared

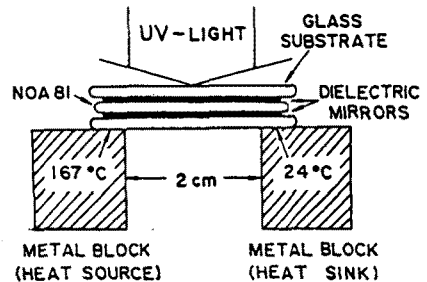


Fig.1 UV-curing process with specific temperature gradient ($7^\circ\text{C}/\text{mm}$).

in this way exhibit the nonlinear transmission phenomena, but we could not observe any nonlinear transmission in the NOA81 etalons UV-cured under a uniform

temperature condition. Maintaining the parallelism between the two mirrors during curing process requires special care. We have prepared two kinds of etalons, S1 and S2.

S1 is made according to the prescription, $(S)(HL)^2(H)(NOA81)(H)(LH)^2(S)$, where (HL) implies a quarter-wave thick $PbCl_2$ as a high index material, H, followed by a quarter-wave thick ThF_4 as a low index material, L. And (S) represents a slide glass substrate. S2 has the structure of $(S)(HL)^2(ZnS)(NOA81)(H)(LH)^2(S)$. The layer (ZnS) in S2 specimen has the optical thickness of $5\lambda/4$. The geometrical thicknesses of NOA81 spacers of S1 and S2 are $15\mu m$ and $18\mu m$, respectively. Fig.2 shows a wavelength dependences of the NOA81 and ZnS absorption coefficients. The absorption coefficient of NOA81 is measured to be very large below 400nm, and low above 400nm.

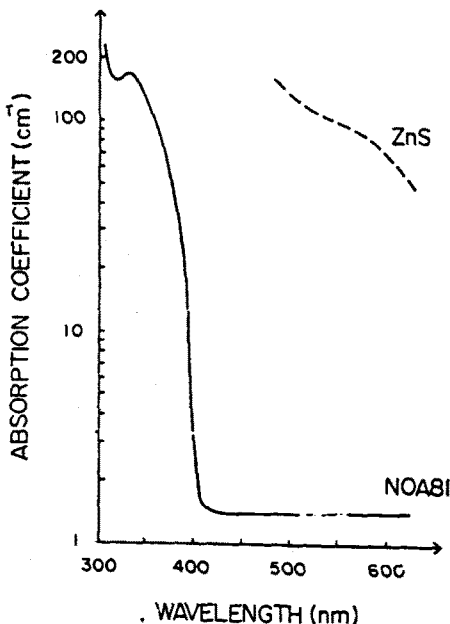


Fig.2 Absorption coefficients of NOA81 (measured in this experiment) and ZnS.

The refractive index of cured NOA81 is 1.56, and its absorption coefficient is $1.5/cm$ at 5145\AA . In the visible region, we see that the absorption coefficient of ZnS thin film is much larger than that of NOA81.

III. Experiments and results

The experimental arrangement is shown in Fig.3. The intensity of cw Ar laser is modulated as a triangular wave of 0.7sec duration by an ADP Pockels' cell modulator. Modulator driver is controlled with a personal computer. The variation of the input power is monitored using a beam splitter and the main beam is focused onto the etalon by a 10X microscope objective. The focal spot diameter is $12\mu m$ which is measured by a knife edge scanning method. The sample is mounted on a rotary mount, and put into the oven to observe the temperature dependent output characteristics. Fig.4 shows the input/output(I/O) characteristics for the various incident angles onto the etalon S1. At normal incidence (0°), S1 has the

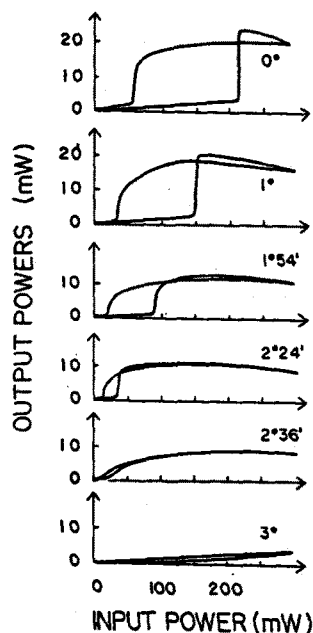


Fig.4 Observed experimental input/output characteristics of the NOA81 non-linear etalon(S1) for various incident angles.

Beam diameter at S1 is $12\mu m$.

largest switch-on power. As the incident angle is increased, the switch-on power decreases. The critical switch-on power for observing the optical bistabilities of S1 is $40mW$ at incident angle of $2^\circ 24'$.

Switching contrast is defined as the ratio of the intensity of the upper branch transmission just after switch-on to the intensity of the lower branch transmission just before switch-on. The observed switching contrast of S1 is 4-8, and this value is better than the largest contrast of 4 observed previously in ZnS or ZnSe interference filters^{2,3,5}. Fig.5 shows the I/O characteristics for the various incident angles on S2 sample. The

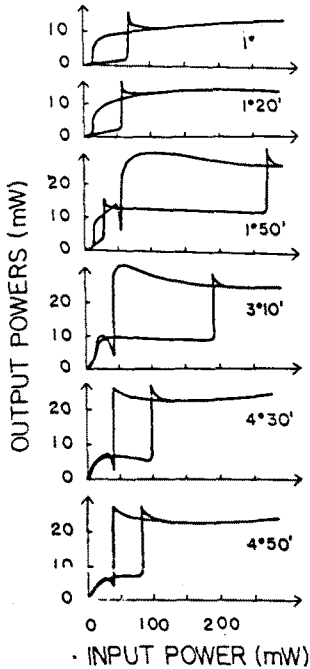


Fig.5 Observed experimental input/output characteristics of the NOA81 nonlinear etalon(S2) for various incident angles.

Beam diameter at S2 is 12 μ m.

switch-on power decreases as the incident angle increases, which is similar to the case of S1. While S1 shows only the first order bistability, S2 exhibits up to the second order bistability, which is due to the fact that S2 has the thicker geometrical thickness and the more effective light absorption for the additional ZnS layer. The decrease of the switch-on power for the increased incident angle as seen in Fig.4 and Fig.5 means that the

nonlinear refractive index change is negative. Fig.6 is the temperature dependence of the transmission in the NOA81 nonlinear etalons. The peaks

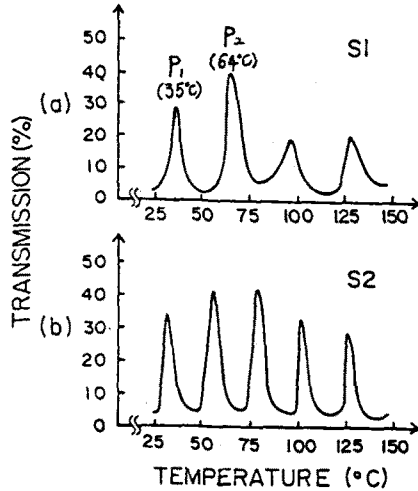


Fig.6 Transmission characteristics of the NOA81 etalons, as a function of the substrate temperature.

(a);sample S1 : (b);sample S2

appearing in Fig.6 represent the cavity resonance states which resulted from the optical thickness change of the spacer due to the temperature increase of the sample. Hence, the separation between the two peaks in Fig.6 corresponds to the phase change of 2π , which is again corresponding to the change in one round trip optical path in the cavity. The cavity phase change may be represented as $4\pi\Delta(nl)/\lambda$, so that

$$4\pi \Delta(nl)/\lambda = \pm 2\pi. \quad \text{---(1)}$$

From the observed fact that increasing the incident angle reduces the switch-on power (Fig.4 and Fig.5), we should choose the negative sign in the right side of eq.(1). Eq.(1) becomes

$$\frac{1}{n} \frac{dn}{dT} + \frac{1}{l} \frac{dl}{dT} = - \frac{\lambda}{2 \Delta T (nl)}, \quad \text{---(2)}$$

where ΔT is the temperature separation between the two peaks in Fig.6 (a) and (b). Putting the experimental values

$\Delta T = 29^\circ\text{C}$, $l = 15\mu\text{m}$ for S1, and $\Delta T = 24^\circ\text{C}$, $l = 18\mu\text{m}$ for S2, we obtain

$$\frac{1}{n} \frac{dn}{dT} + \frac{1}{l} \frac{dl}{dT} = -3.8 \times 10^{-4} / ^\circ\text{C}$$

for both of S1 and S2. Because dl/dT is positive, we may conclude that the thermo-optic coefficient dn/dT of NOA81 has the negative sign and its magnitude is at least $3.8 \times 10^{-4} / ^\circ\text{C}$. Fig.7 shows the I/O characteristics of S1 for the various temperatures at incident angle 0° . As

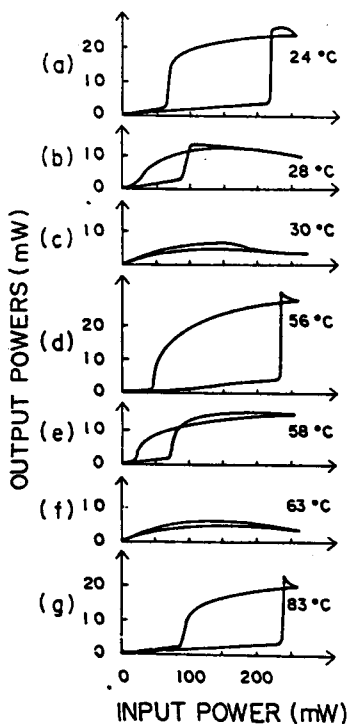


Fig.7 The input/output characteristics of the NOA81 etalon(S1) for the various substrate temperatures.

the substrate temperature approaches to 34°C from the room temperature of 24°C , the initial cavity state shifts toward the first resonance state P_1 of Fig.6(a), so that the switch-on power becomes smaller (Fig.7(a)-(c)). For the further increase of temperature, the higher resonance state P_2 of Fig.6(a) appears again, and the similar I/O characteristics repeat as shown in Fig.7(d)-(g). From the

above results, it can be seen that the increase of the temperature can tune the cavity state repeatedly, and the origin of the nonlinearity in NOA81 is thermal effect.

Fig.8 shows the switch-on time vs. the input power ratio P_{in}/P_{on} , where P_{in} is the input power and P_{on} is the switch-on power. It can be seen from Fig.8 that

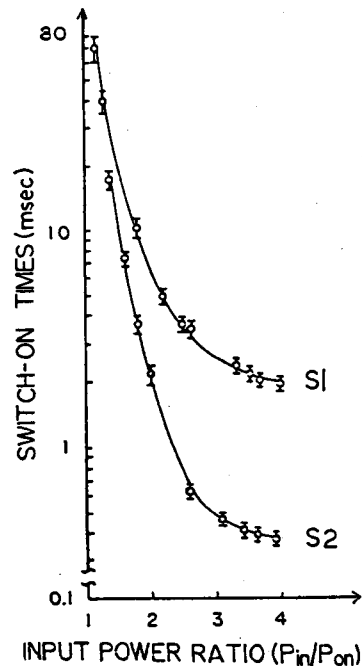


Fig.8 Measured switch-on time as a function of P_{in}/P_{on} . P_{in} ; the input power; P_{on} ; the switch-on power. Beam diameters at S1 and S2 are both $12\mu\text{m}$.

the switch-on time becomes longer as the input power ratio approaches to 1 ($P_{in}/P_{on} \rightarrow 1$). This behavior of NOA81 etalons corresponds to the critical slowing down phenomenon already observed in many bistable devices^{6,7}. The reason why the switch-on time of S2 is faster than that of S1 is that S2 has the additional absorption layer of ZnS, and that the switch-on time is inversely proportional to the absorption⁴. The shortest switch-on time of NOA81 etalons in this experiment is measured to be $350\mu\text{sec}$ for S2, and 2msec for S1.

VI. Conclusions

The etalons filled with NOA81 optical adhesive UV-cured with the specific temperature gradient $7^{\circ}\text{C}/\text{mm}$ exhibit the reproducible optical bistabilities at 5145\AA for the various temperature range.

The etalons UV-cured in a uniform temperature environment do not show any bistability. Curing process with a lateral temperature gradient gives the optical bistability to the etalon.

Continuing works on the temperature gradient effect are in progress in this laboratory. The switch-on time and the switch-on power are expected to improve further by selecting a proper absorption layer and the curing condition such as temperature gradient.

References

- (1) S.D.Smith, Appl.Opt., 25,1550- (1986).
- (2) S.D.Smith, A.C.Walker, B.S.Wherrett, F.A.P.Tooley, N.Craft, J.G.H.Mathew, M.R.Taghizadeh, I.Remond, and R.J.Canbell, Opt.Eng., 26, 45- (1987).
- (3) M.T.Tsao, L.Wang, R.Jin, R.W.Sprague, G.Gigioli, H.M.Kulcke, Y.D.Li, H.M.Chou, H.M.Gibbs, and N.Peyghambarian, Opt.Eng., 26,41- (1987).
- (4) G.R.Olbright, N.Peyghambarian, H.M.Gibbs, H.A.Macleod, and F.V.Millign, Appl.Phys.Lett., 45, 1031- (1984).
- (5) Y.T.Chow, B.S.Wherrett, E.V.Stryland, B.T.McGuckin, D.Hutchings, J.G.H.Mathew, A.Miller, and K.Lewis, Appl.Phys.Lett., 45, 1031- (1984).
- (6) I.Janossy, J.Gordon, H.Mathew, E.Abrahm, M.R.Taghizadeh, and S.D.Smith, IEEE.J.Quantum Electron, QE-22, 2224- (1986).
- (7) H.M.Gibbs, Optical Bistability : Light Controlling with Light, Academic press, New York. 221-229 (1985).

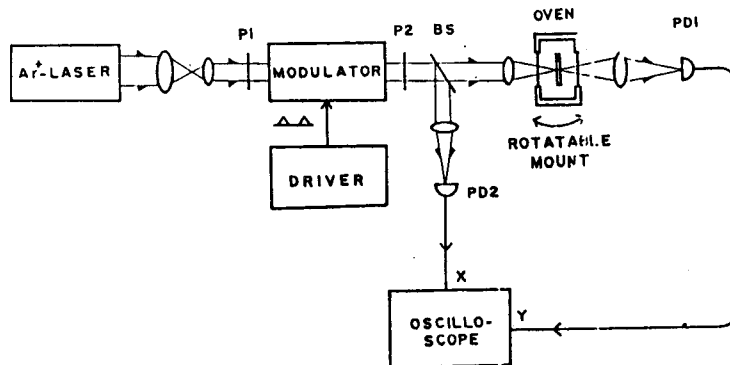


Fig.3 Experimental arrangement for observation of the optical bistabilities in NOA81 nonlinear etalons. P1,P2 ; linear polarizers: PD1,PD2 ; photodiodes: BS ; beam splitter.